Journal of Mechanical Engineering Research and Developments
ISSN: 1024-1752
CODEN: JERDFO
Vol. 44, No. 4, pp. 123-133
Published Year 2021

Implementation of Three Phase Split Source Inverter (SSI) using SIC MOSFETs and VFD for Solar Irrigation Application

Omar Hasan Mohammad and Thamir Hassan Atyia*

Electrical Engineering, Tikrit University, Iraq

*Corresponding Author Email: dr.thamir.atyia@tu.edu.iq

ABSTRACT: The rapid growth and the large set up towards the use of renewable energy resources leads to an increase in research and studies. In this research study the introduction of new technologies with the purpose of increasing the efficiency of the solar powered water pump for agriculture usage and making it practical. The design and practical implementation of STM32F334R8T6 microcontroller board a based Space Vector Pulse Width Modulation (SVPWM) for a three-phase inverter to control the speed of a three-phase Induction Motor (IM) was accomplished. The control is achieved via varying the stator voltage and varying frequency with V/F control method. The inverter is employed a three phase Split Source Inverter (SSI) to generate the appropriate PWM signals for the inverter switches. The software program was developed using C language. Silicon Carbide metal–oxide–semiconductor field-effect transistor (SIC MOSFETs) was used as switches of transistors' gates control, and SVPWM techniques used to control the speed of a three-phase Induction Motor (IM), using STM32F334R8T6 microcontroller , A three-phase Induction Motor (IM) capacity of 0.5 hp was operated on the inverter that was implemented and readings of the system's performance practically operated were recorded, including measuring the motor speed for different conditions during the change of solar radiation during the day. The designed system implemented practically and performed well even with partial cloudy weather the system was capable of running the water pump with the obtained solar power and the water flow rate varies during the day depending on amount of solar radiation. Also, MATLAB/SIMULINK software was used for simulation and verification of the practically built system and comparison between experimental and simulation results have been inducted.

KEYWORDS: DC-AC, Pulse Width Modulation, Single-stage, Space Vector, Split-Source Inverter, STM32, Solar powered water pump, Z source inverter.

INTRODUCTION

Advance in power electronics has led to an increased interest in three-phase Inverters with Pulse Width Modulation (PWM) control Space Vector Modulation(SVPWM) [1] and [2]. PWM technique aim at generating a sinusoidal inverter output voltage without low-order harmonics. The most widely used in motor drive and industrial applications are the space vector PWM. Most PWM techniques are developed using modern digital control circuits, where reprogramming of the carrier frequency and reference frequency are possible [3]. A new attractive single unit DC-AC power converter topology called split-source inverter (SSI) was proposed due to its good features in terms of size, cost, weight and simplicity of the system. SSI is a combination of boost stage and VSI stage as single unit DC-AC power converters which have some merits compared to other equivalent topologies [4]. The main merit of SSI being the use of same modulation schemes of the conventional VSI without any modification, and required less component compare with ZSI. There are various kinds of PWM techniques available such as Space Vector Modulation (SVM), and Sinusoidal Pulse Width Modulation(SPWM). All these techniques aim to generating a sinusoidal inverter output voltage with low-order harmonics [5]. STM32 electronic board to drive the electronics SIC MOSFETs switch [3], for the inverter were used to implement PWM techniques and can be compared between switching devises [6].as a application of this project scheme comprises of pump energetic by 3-phase IM Virtual reality are completed in MATLAB/ Simulink [7], outcomes showed that PV structure .discuses Advanced Irrigation System describes how the underground water can be collected by Solar Photovoltaic(SPV) Systems for remote areas , uses the induction motor to utilize the underground water PV system for running the system making (SPV) the most economical. Solar pumping decreases the electric charges and saves the money, which can be used in other schemes, the submersible pump and equipment have low maintenance cost and running cost making the system more suitable and ecofriendly [8] .

Maximum power point tracing(MPPT)

To enhance efficiency of the renewable energy system, it is necessary to track the maximum power point of the PV array. The PV array has a unique operating point that can supply maximum power to the load. This point is called the maximum power point (MPP). The locus of this point has a nonlinear variation with solar irradiance, the cell temperature, and other effects. Thus, in order to operate the PV array at its MPP, the PV system must contain a maximum power point tracking (MPPT) controller and its flow chart is depicted in figure (1). The maximum power point (MPP) is obtained when the derivative of PV power by the voltage (dPpv/dVpv) is zero. Basically, to achieve the maximum power point of operation, the generator voltage Vpv is regulated so that it increases when the slope dPpv/dVpv is positive and it decreases when the slope dPpv/dVpv [9].

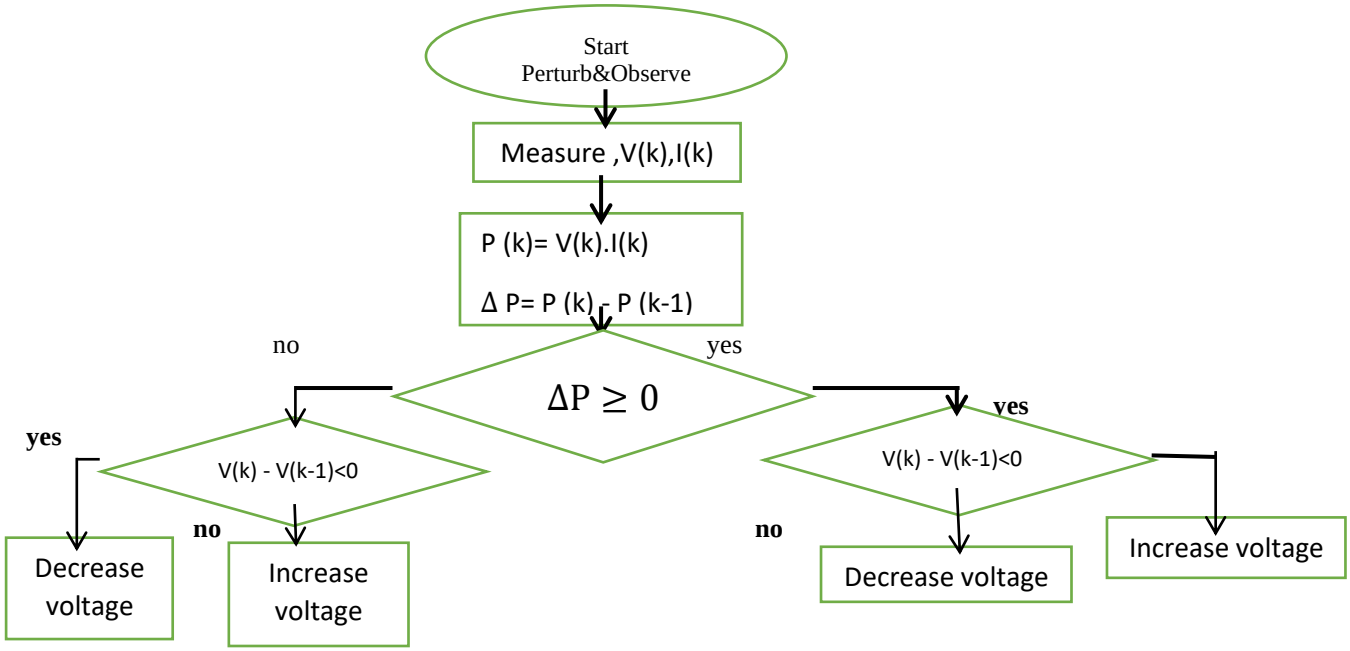

Figure 1. Flowchart of Perturb & Observe algorithm

Three phase Split Source Inverter (SSI)

A new single unit DC-AC converter topology called split-source inverter (SSI) as shown in figure (2) compound of two unit conversion, the single unit DC AC is congregated higher attention due to its less weight, lower size, and simplicity. Especially when SIC MOSFETs used as an electronic switches for inverter would have advantages such as extremely low losses , higher switching frequencies, and SIC MOSFETs compound of build in flywheel diodes utilized to decrease passive component compared to the ZSI, addition to have a diode for each legs of SSI [4]. Benefits of SSI topology are constant inverter voltage, continuous input current with a low frequency component and a normal approach employs same eight states of VSI. AC output voltage is greater than input voltage, in various type of DC-AC power conversions.

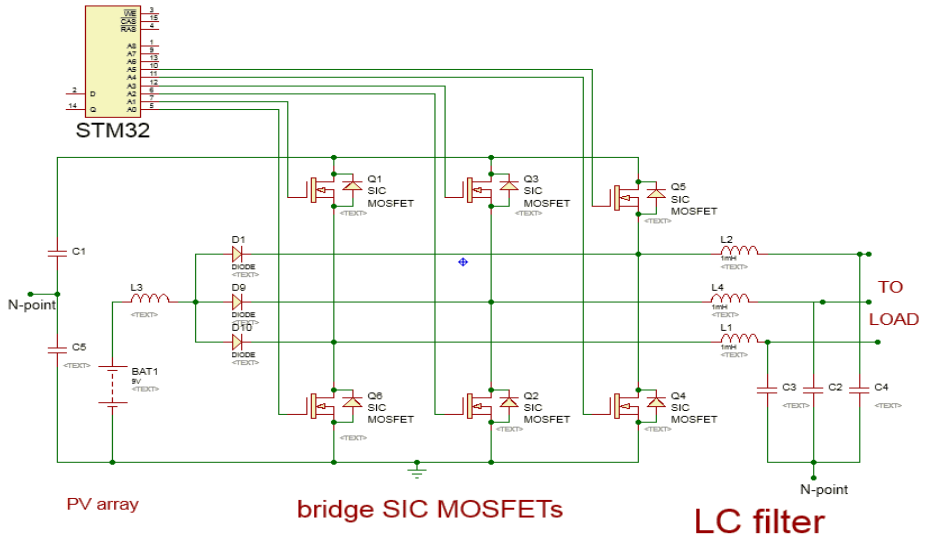

Figure 2. Proposed three-phase split source inverter (SSI)

If the voltage source inverter (VSI) is consider, then additional DC-DC boosting stage required to eliminate the step-down which is considered as one of VSI limitations. The main features and benefits of the Silicon Carbide Power MOSFET are: Very high temperature handling capability, Significantly reduced switching lossesLow on-state resistance (20 mΩ) , Very fast and robust intrinsic body diode and Reduce switching losses using SIC MOSFETs [10].

Mathematical Derivation

inductor is charge depend on duty cycle (D) and this not fixed [4]

$$D = \frac{t_{on}}{T} \ldots\ldots\ldots \quad (1)$$

$$T = t_{on} + t_{off}$$

Where T = Total inductor charging and discharging time during one switching cycle.

ton = the inductor charging time, toff = the inductor discharging time.

SVPWM Scheme: driven to eight switching states where the inverter has six active states (1-6) and two zero states (0 and 7) [11] The inductor L of the SSI is charged with a duty cycle D , For the SVPWM scheme discussed in , considering the modulation index M definition, Where D is related to M by [12].

$$D(\theta) = \frac{1}{2}\left\{1 - Msin\left(\theta - \frac{2}{\Pi}\right)\right\} \quad \ldots\ldots\ldots \quad (2)$$

Where $0 \leq \theta \leq \frac{\pi}{3}$ Based on eq (2) , the duty cycle D is not constant , as it varies with a low frequency The duty cycle variation of the SVPWM is bounded by D_{min} and D_{max} given by [12]

$$\boldsymbol{D_{min} = 0.5 + \frac{\sqrt{3}\,M}{4}} \quad \ldots\ldots\ldots \quad (3)$$

$$\boldsymbol{D_{max} = 0.5 + \frac{M}{2}} \quad \ldots\ldots\ldots \quad .(4)$$

The inductor is charged with an average duty cycle D_{av} given by [12]

$$\boldsymbol{D_{av} = 0.5 + \frac{3M}{2\pi}} \quad \ldots\ldots\ldots \quad (5)$$

Based on the inductor flux balance and the capacitor charge balance, the normalized average inverter voltage is $\frac{V_{inv}}{V_{DC}}$ given by [4]

$$\frac{V_{inv}}{V_{DC}} = \frac{1}{1-D_{av}} \quad \ldots\ldots \quad (6)$$

where, VDC is the input DC voltage. Substituting (5) in (6) yields

$$\frac{V_{inv}}{V_{DC}} = \frac{2\pi}{\pi-3M} \quad \ldots\ldots \quad . \quad (7)$$

From (2-29), the normalized output fundamental peak phase voltage $\frac{V_{\emptyset 1}}{V_{DC}}$ is

$$\frac{V_{\emptyset 1}}{V_{DC}} = \frac{2\pi M}{\sqrt{3}\,\pi - 3\sqrt{3}\,\pi} \quad \ldots\ldots \quad (8)$$

Finally, the selection of the inductor should consider the high frequency and the low frequency current components due to the switching and the duty cycle variation respectively. This is done by finding high frequency ripple for the inductor current =ΔI_{Lh} and the capacitor voltage ΔV_{invh} given by [12]

$$\Delta I_{Lh} = \frac{DV_{DC}}{f_s L} \quad \ldots\ldots \quad (9)$$

$$\Delta V_{invh} = \frac{(1-D)I_{DC}}{f_s C} \quad \ldots\ldots \quad (10)$$

The low frequency inductor voltage ripple, assuming constant inverter voltage, is given by

$|V_{L_l}|$=(1-D(θ))V_{inv} , while the low frequency capacitor current ripple, assuming constant inductor current , is given by $|I_{c_l}|$=(1-D(θ))I_{DC} Now, in order to estimate the low frequency ripple components, only the fundamental terms of $|V_{L_l}|$ and $|I_{c_l}|$ are considered, which are proportional to the fundamental term of Fourier series of D(θ) [12]

$$D_l = \frac{6M}{35\pi} \quad \ldots\ldots \quad (11)$$

$$\Delta I_{Lh} \approx \frac{D_l V_{inv}}{6w_1 L} = \frac{MV_{inv}}{70\pi^2 f_1 L} \quad \ldots\ldots \quad (12)$$

$$\Delta V_{invl} \approx \frac{D_l I_{DC}}{6w_1 C} = \frac{MV_{inv}}{70\pi^2 f_1 C} \quad \ldots\ldots \quad (13)$$

Under worst conditions, the low frequency ripple is added to the high frequency one required inductance and capacitance are given by [12]

$$L \approx \frac{MV_{inv}}{70\pi^2 f_1 \Delta I_L} + \frac{D_{max} V_{DC}}{f_s \Delta I_L} \quad \ldots\ldots \quad (14)$$

$$C \approx \frac{MI_{DC}}{70\pi^2 f_1 \Delta V_{inv}} + \frac{(1-D_{min})I_{DC}}{f_s \Delta V_{inv}} \quad \ldots\ldots \quad (15)$$

ARCHITECTURES PROPOSED FOR GENERATE PWM

A.SVPWM in STM32The SVPWM technique is more popular than conventional technique especially for driving machine applications, because of its exceptional features: More efficient use of DC supply voltage, more output voltage then traditional modulation, lower Total Harmonic Distortion (THD), and less co

SVPWM IPLEMENTATION

The space vector PWM can be implemented following steps as presented in figure (3):

Step1. Determine Vd, Vq, Vref, and angle (α) figure (3)
Step2. Determine time duration T1, T2, T0
Step3. Determine the switching time of each switches

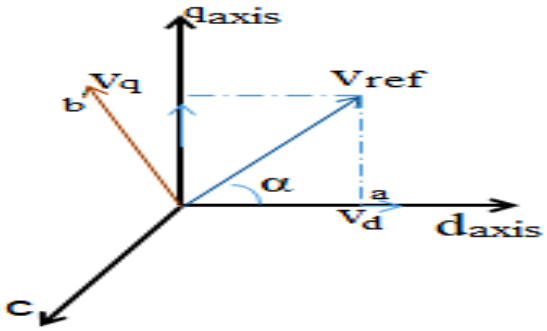

Figure 3. Voltage Space Vector and its d, q axis

STM32 microcontroller Based PWM Control for Variable Voltage Control In order to calculate the duty cycle (D) for each phase after taking frequency of dq0, then calculate the dq0 for each phase, and use High Resolution Timer (HRTIM) to generate 6 signals for each of the two vice versa signals (each two complementary) and each two complementary signals between the dead time, and then multiply by a parameter whose value depends on the speed specified or identified by the MPPT controller algorithm so that the parameter value is equal to the value of the speed specified in advance by the programmer (variable speed variable frequency) to the ratio of the rated speed. To calculate the duty cycle for each phase after taking Vdq0. for calculating the duty cycle for each phase, and then use HRTIM to generate 6 signals. Every two signals for one phase (every two complemented) and every two complementary signals between them are dead time (each two signals have a dead time), be calculated the dead time at last step. From above process by multiply the parameter(index(modulation)) whose value depends on the specified speed is limited by the controller MPPT, so that the coefficient (M)value is equal to the value of the specified speed lastly by the programmer (N ref) to the ratio of the rated speed(N rated). The aim of this architecture is to feed the IM with a variable stator voltage by changing the modulation index (slope), and states of switching of the inverter. The whole design process is presented in figure (4).

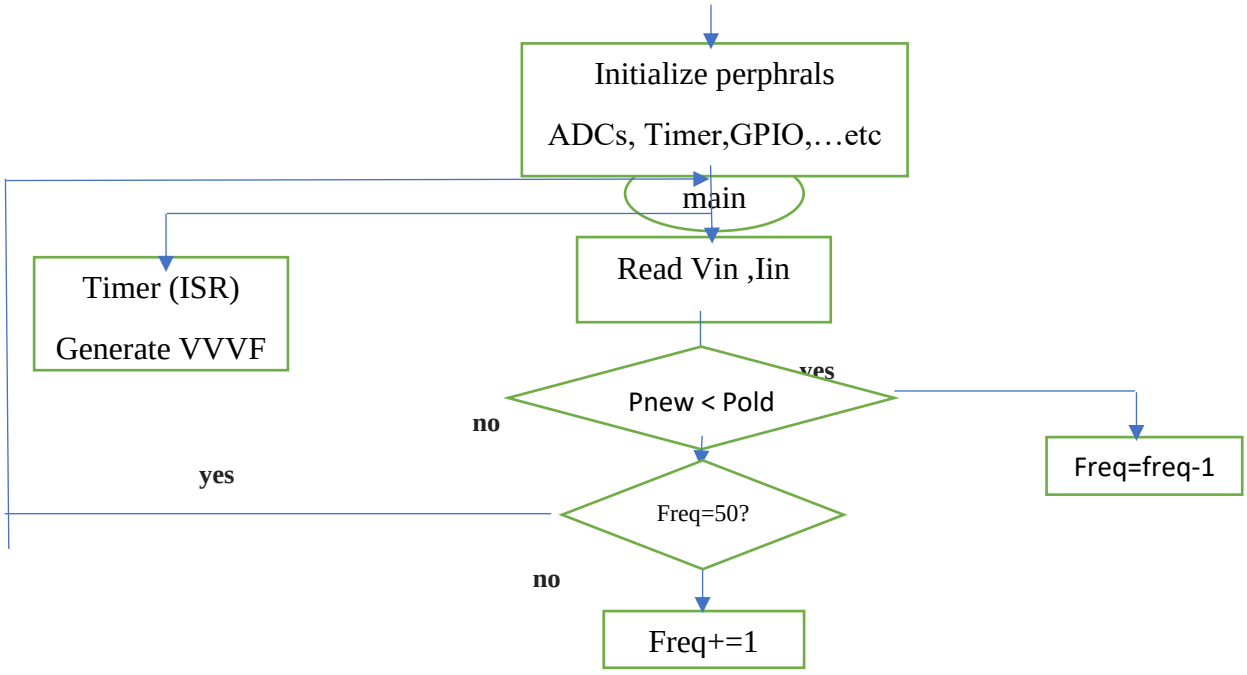

Figure 4. Flow chart process and software designs

Voltage Frequency ratio (V/F) control of AC Motor

Normal start of a motor require high torque which draws current surges up to 10 times the full-load current. In contrast, variable-frequency drives enable "soft start", gradually ramping up a motor to the operating speed. This reduces the

mechanical and electrical stress on the motor thus bringing down the maintenance and repair costs then prolongs the motor life. A variable frequency drive can result in significant energy savings. For machines even a small reduction in motor speed will highly leverage the energy savings. A variable frequency drive controlling a pump motor makes it run at a speed less than full speed and this can substantially reduce energy consumption as compared to a motor running at constant speed for the same time duration [13] & [14].

Practical Implementation

The solar panels were installed as shown in figure (5) the pictures below, and the number of these panels is eight that they were installed in the form of two series for each series 4 panels linked in series to become the total voltage of 122.4 volts because the working voltage for each panel is 30.6 volts Panel installation: 2KW solar cell system specification shown in figure (5)

Figure 5. Shows the installation of the solar panel

Generation of PWM using High Resolution Timer

The PWM switching frequency of 30 KHz have been selected and set up the HRTIM pre-scale to 0 (no division to the system clock), this means that the input clock of the timer is 512 MHz, therefore, the timer period would be:

$$Timer\ Period = \left(\frac{\text{System Clock}}{\text{PWM Frequency}} - 1\right) = \left(\frac{512\text{MHz}}{30\ \text{KHz}} - 1\right) = 15065.6 \qquad \ldots. (16)$$

the meaning if 100% PWM is required to be created, favorites output comparison register should be established to level of 15065, in same way if 50% PWM is required to be generate then the compare register should be set to value of 10999 to the other.. shows how to produce PWM signals.

In the formed, six PWM output pins are require to drive the lower, and upper SiC MOSFET's , so the HRTMR is selected for this work which has channels of PWM outputs. HRTMR Ch1-Ch3 (Pins 40,42, and 44 on the Microcontroller) were used to drive the three upper MOSFET's and HRTMR Ch1n-Ch3n complementary channels (Pins 39, 41, and 43 on the Microcontroller) were used to drive the three lower MOSFET's. The count required to generate sample for carrier frequency of 30 KHz ,and sine wave frequency 50 Hz as shown:

$$PWM\ Samples\ Count = \frac{30\text{Khz}}{50\text{Hz}} = 600\ Samples/Cycle \qquad \ldots\ldots \qquad (17)$$

Using HRTIM software to produce a PWM signals at the six output pins of inverter (the upper and lower halves of the bridge).The signals must be complementary on each inverter leg (i.e. the upper signal is exactly the inverted lower signal with small dead-time insertion to avoid cross-conduction).We also must configure the timer to generate an interrupt at each PWM cycle (1/30KHz=33.3 micro second) to use it for updating the capture compare register with data from the look-up table is generated by programing code .

Reading the DC input and inverter dc-bus output

Any closed-loop controller must be able to read the plant's output and then set the plant's input accordingly to maintain the output at the desired value.

SIC MOSFETs Driving

We used the SIC MOSFETs driver topology in the design of the driver which means we need -6,0, 18V isolated voltages(One power source for each upper SIC MOSFETs, and one for the three lower SIC MOSFET's and control circuit) so we designed an SMPS (Switch Mode Power Supply) that will be explained. The SIC MOSFETs driver IC that we used is HCPL-316J, which has opto-isolated independent drivers. We used six IC's to drive the six SIC MOSFETs Bridge; each IC is used to drive one leg (one upper or one lower SIC MOSFETs).

Protection Circuit

The protection circuit was designed to provide protection for the SIC MOSFETs from overcurrent and overvoltage. The protection is done by the insulator through port No. 14 in the insulator circuit. It consists of op-amps functioning as comparators, one for voltage sensing and one for current sensing. The current comparator (current transducer) compares the voltage (inverting input) across the shunt resistor (the current flows in the bridge passes through the shunt resistor and produces a voltage that is proportional to the amplitude of the current) with a reference voltage on the non-inverting input. if the inverting input goes higher than the reference voltage, the comparator outputs goes low which in turn, will disable all the SIC MOSFETs drivers and shuts them down .the isolation circuit generates 18 volts, using a voltage regulator (Zener diode) in order to obtain a voltage of 7 volts as shown in driver board. It is connected to the collector of the transistor to be protected and a resistance is placed in series to determine the current, whose value is calculated as shown in addition to 3 diodes respectively Consequently, its resistor will be sensitive to a voltage of 3 volts or more .

The output LC filter

Since the output voltage of the inverter without an LC filter is a Quasi-sine wave, it is not suitable to operate electrical equipment directly to this type of waveforms (other than motors). Therefore, we must use LC filter in order to get a pure sine wave. The inductor of the output LC filter should have a toroidal core with material that have a low loss, relatively high saturation level and capable of operating at high frequencies. We chose the very popular material ideally suited for this type of applications known as "Kool Mu "material. The part number of the toroidal core we used is the Micrometals.6.5% silicon iron alloy with distributed air gap high saturation flux density, lower losses iron core, good temperature stabilization.
In order to get a 1.2 mH from this core, we must ensure that the DC magnetizing force (H) is less than the limit of this core. The first thing we do is determining the number of turns required to get 1.2 mH inductance at 2.5A load. Firstly, we calculate the DC Energy Storage in the inductor:

J= $\frac{1}{2} L * I^2$ = 3750µJo

NI is about 400 (ampere turns) and the required number of turns is equal to $\frac{NI}{I} = \frac{400}{2} \approx 200$ turns .The capacitors of the LC filter is normally about 1uF star-connected polyester film type (Non-polarized)

The SSI inductor

From the simulation results, the minimum inductance value is about 5mH at 900W output load. The input current of the inductor is 5A so the $\frac{1}{2} LI^2$ value is in µJ and it is a relatively large value and requires a big (and expensive) core so we need to determine the minimum core size that can handle such a value. The Micrometals PPF250040 is the smallest part number that meets our requirements. From the core datasheet the required NI ampere turns, and The AL Value at this given NI to find number of turns N = NI/I = 180 turns.

Power supply design

Because we used the isolated SICMOSFETs, and IGBT driver topology for the inverter, we need isolated power supplies between 12V and 18V at a rated current of about 1A for each voltage. In addition, we need 123V supply with a capability of at least 5A to use it as the DC input voltage for the SSI inverter.

SMPS Transformer design

For this amount of power (about 900W), the best topology suited for this purpose is the half-bridge switching mode power supply. 50 KHz operating frequency of the power supply will be used, and IR2085S the IC controller will be used. A constant voltage of 12 or 15 volts is obtained by connecting a Zener voltage regulator to a diode. Fortunately, the main source is from solar panels, which is a constant voltage, or the amount of voltage can be obtained through an external power supply as shown in the figure, which can be designed through steps next. We use core has large wire area of all core styles is ETD. Needed for all additional layers of insulation. No air-gap is needed for IGBTs forward-mode converters. The core material is going to be PC40 (TDK). This material will yield possible core losses at frequency known. Valuation core size suitable for this application is ETD49 when calculating the number of turns for the primary, one need to consider the initial start-up condition, which places the full input voltage across the primary winding for the first few milliseconds of operation. We must be assured that the transformer will not enter saturation during this period. The transformer design conditions become the maximum specified ambient temperature and the highest specified ac input. The number of primary turns needed for the primary winding will be:

$$Npri = \frac{Vin(nominal)*10^8}{4*f*Bmax*Ac} \quad , \quad Npri = \frac{193V*10^8}{4*50KHz*2000G*2.11cm^2} = 22.8\,Turns \approx 23$$

$$Nsec = \frac{1.1(Vout+Vfwd)*Npri}{(VINmin)*Dmax} \quad , \quad Nsec = \frac{1.1(15+1.2)*18}{(97)*0.94} = 3.49\,Turns \approx 4$$

The ESP8266 Wi-Fi Module

We designed the microcontroller driver board to be remotely controlled and monitored. When we connect the board with any Wi-Fi enabled device such as smartphone or laptop we can perform basic tasks like starting the inverter SVPWM mode, stopping the inverter, reading the DC input voltage, reading the inverter DC voltage and the current modulation index. The ESP8266 Wi-Fi Module is a self-contained SOC (System-On-Chip) with protocol TCP/IP stacking can be given any access of microcontroller to Wi-Fi networks. The ESP8266 is capable of either hosting an application or offloading all Wi-Fi networking functions from another application processor. Each ESP8266 module comes pre-programmed with a command set firmware, which means that we must re-program it to suit our applications. We programmed the ESP8266 to act as simple uart (universal asynchronous receiver transmitter) to TCP/IP or simply TCP to serial, which means that the ESP8266 is connected to the microcontroller's uart (via RX and TX pins) and passes any incoming data from the microcontroller to a TCP server (TCP/IP port 23) and receives any incoming data from the TCP server and redirect it to the microcontroller via the RX pin of the microcontroller. This means that we created virtual wires connecting the microcontroller with smartphone or laptop. component of SSI as shown in Table (1) below.

Table 1. Parameters of SSI

VDC	IDC	Vϕ1	Pf	Iϕ1	fs	f1	C input (µF)	Lfilter (mH)	Cfilter (µF)	Vin	D		L	C
										(V)	Dmin Dmax	Davg	L (mH)	C (µF)
122V	20 A		0.85lag		30 KHz	50	1500	1	1	344	0.67 0.85	0.79	5	280

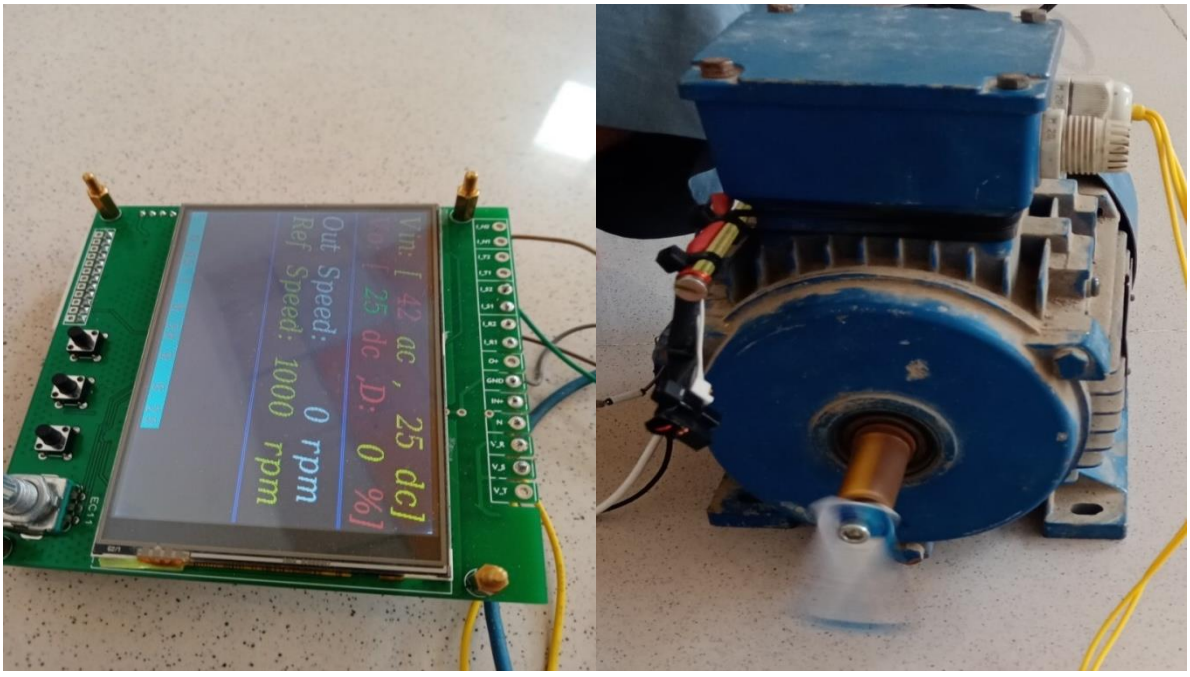

Figure 6. the speed measuring process

Figure 7. the three-phase SSI-inverter (top and side) view

10: the Results of STM32microcontroller Based on SVPWM Control via V/F Control Strategy for Scheme for VVVF

The table and chart below table (2),and figure (8) represents the practical results of controlling the speed of a three-phase induction machine Using the maximum power point tracking.

We note from the table that the relationship between machine speed, voltage and frequency is linear velocity, and by obtaining this feature we will be able to obtain the values of voltage and frequency in a fixed proportion that are directly proportional to each other on the rotating part of the machine and this is a technique in VFD ,Whereas, by changing the

value of the power generated from the solar panels, by using the programming the value of each of the voltage frequency changes, thus the value of the machine speed changes because the value of the magnetic flux on the rotating part of the machine is the result of dividing the voltage into the flux frequency is a constant value. Therefore, this enables us to track the maximum point of the solar radiation electrically using programming thus we can make the maximum use of the solar radiation for the purpose of operating the machine for the purpose of solar irrigation**.** Table shown below illustrate variable voltage and frequency on the stator of the machine by using V/F strategy applied

Supply Frequency (Hz)	**Stator Voltage (V)**	**Synchronous speed (rpm)** ($N_m = \frac{120*f}{p}$)	**Actual Speed (rpm) (as measured**
5	31	100	99
10	52	200	199
18	105	360	361
25	127	500	498
30	152	600	598
35	179	700	698
40	203	800	798
45	228	900	898
50	251	1000	997

Table 2. Results of V/F control of the IM

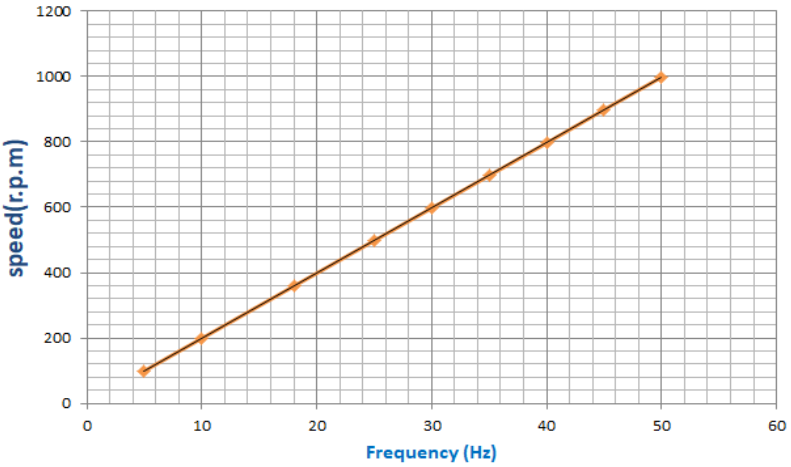

Figure 8. relation between frequency, and rotor speed

CONCLUSIONS

- The amount of solar radiation changes during the day
- With an increase in the amount of radiation, the power generated will increase, thus increasing the machine's operating speed, which will increase the speed of the machine.
- The higher switching frequencies give the best Total Harmonic Distortion (THD) value therefore we get pure sine wave is comfortable for loads.
- When using SIC MOSFETs, we can use high switching frequencies, thus reducing the size of the coils' values used in the inverter and heat sinks.
- STM32F334R8T6 MICROCONTROLLER supports the use of sic mosfet as it generates control pulses at the gate at high frequencies equal to 480 mhz, it is also implemented programmatically in easy programming language(C language) is suitable for solar system application MPPT & VFD
- SVPWM used in control gate pulses is proportional with Clark & Park Transformation (abc - αβ and abc - dq0) there are suitable for V/F control (Because it enables us to know the voltage on the machine, the magnitude and angle at any point we want it. In other ways, we need to pass a full cycle of the wave in order for us to calculate the voltage rate. Therefore, it is suitable for controlling the machine's speed because the machine's speed is nonlinear and must be dealt with momentarily.

- The speed of machine is directly proportional to the voltage and the power generated by the panels, so the starting torque can be controlled and the starting is flexible.
- Used Perturb & Observe method for MPPT more simple and suitable.
- Solar irrigation reduce cost by it dispensing of the charging system (batteries)

REFERENCES

[1] A. T. Mohsin and I. M. Abdulbaqi, "Analysis of an Irrigation Pump Driver Fed by Solar PV Panels (Part II)," *Int. Iraqi Conf. Eng. Technol. its Appl. IICETA 2018*, pp. 124–129, 2018, doi: 10.1109/IICETA.2018.8458080.

[2] R. Parmar, V. Gupta, and B. Kumar, "PERFORMANCE COMPARISON BETWEEN PWM AND SVPWM," vol. 1, no. 3, pp. 26–30, 2014.

[3] W. Hsu, J. Fang, and C. Huang, "Design of Photovoltaic Inverter Based on STM32 Microcontrollers," 2019, doi: 10.1088/1757-899X/644/1/012013.

[4] P. Yadav, A. K. Sharma, and S. Garg, "Performance analysis of three-phase split source inverter," *Proc. - 2016 Int. Conf. Micro-Electronics Telecommun. Eng. ICMETE 2016*, vol. 2, no. 2, pp. 504–507, 2016, doi: 10.1109/ICMETE.2016.71.

[5] P. T. Engineering and P. T. Ibraheem, Engineering, "FPGA Based Three-Phase Sinusoidal PWM Control for Voltage Source Inverter Fed IM ةيتلوف سكاع ىلع ةرطيسلل ايلقح ةجمربملا تاباوبلا ةفوفصم مادختسا يثح كرحم ةيذغتلا يبيجلا ةضبنلا ضرع نيمضت قيرط نع روطلا يثلاث," 2010.

[6] Y. Liu, S. Jiang, D. Jin, and J. Peng, "Performance comparison of Si IGBT and SiC MOSFET power devices based LCL three-phase inverter with double closed-loop control," *IET Power Electron.*, vol. 12, no. 2, pp. 322–329, 2019, doi: 10.1049/iet-pel.2018.5702.

[7] F. Alkarrami, T. Iqbal, K. Pope, and G. Rideout, "Dynamic Modelling of Submersible Pump Based Solar Water-Pumping System with Three-Phase Induction Motor Using MATLAB," *J. Power Energy Eng.*, vol. 08, no. 02, pp. 20–64, 2020, doi: 10.4236/jpee.2020.82002.

[8] B. Bhattacharjee, A. Chakrabarti, and P. K. Sadhu, "Solar Photovoltaic Integrated Pump for Advanced Irrigation System," no. 8, pp. 3246–3250, 2019.

[9] H. Machrafi, *Green Energy and Technology*. 2012.

[10] N. E. Mode, "C2M0045170D Silicon Carbide Power MOSFET," pp. 1–10, 2016.

[11] P. H. Tran, "MATLAB / SIMULINK IMPLEMENTATION AND ANALYSIS OF THREE PULSE-WIDTH-MODULATION (PWM)," no. May, 2012.

[12] A. Abdelhakim, P. Mattavelli, and G. Spiazzi, "Three-Phase Split-Source Inverter (SSI): Analysis and Modulation," *IEEE Trans. Power Electron.*, vol. 31, no. 11, pp. 7451–7461, 2016, doi: 10.1109/TPEL.2015.2513204.

[13] K. Unni and S. S. Thale, "Design and Development of a Solar PV Inverter for Water Pumping Applications," pp. 1–6, 2015.

[14] M. Pradesh, "Simulation and Analysis of Space Vector PWM Inverter Fed Three Phase Induction Motor Drive," vol. 1, no. 10, pp. 299–308, 2016.